



BRIDGE PROTECTION SYSTEMS ATTACHMENT

FHWA FSK Bridge Main Span Pier Lateral Capacity

Baltimore, MD

DCA24MM031

(17 pages)

**Francis Scott Key Bridge Collapse Investigation:
Main Span Pier Lateral Capacity**

Prepared For:

National Transportation Safety Board
(NTSB Accident ID: DCA24MM031)

By:

Federal Highway Administration
Office of Bridges and Structures

November 7, 2024

TABLE OF CONTENTS

Federal Highway Administration (FHWA) Role	4
Report Purpose	4
Analysis Methods	4
Loads	4
Dead Load	5
Live Load	5
Application of loads	5
Limit states and load and resistance factors	6
Material properties	7
Concrete and Steel	7
Foundation soils	7
Member capacities	9
Column flexural capacity – linear-elastic model	9
Column flexural capacity – nonlinear model	10
Column shear capacity	12
Pier capacity Calculations	13
Linear-elastic modeling	13
Nonlinear modeling	14
Foundation Capacity Calculations	15
Discussion and reported capacities	16

LIST OF FIGURES

Figure 1. Axial load-moment diagram, Piers 16 and 19 section with void	10
Figure 2. Axial load-moment diagram, Piers 17 and 18 section with void	10
Figure 3. Moment-curvature relationship for Piers 16 and 19 at axial load, P = 4,088 kips	11
Figure 4. Moment-curvature relationship for Piers 17 and 18 at axial load, P = 7,951 kips	11
Figure 5. As-built drawing of Pier 18 showing column construction joint (noted “C.J.”).....	12

LIST OF TABLES

Table 1. Concrete properties	7
Table 2. Reinforcing steel properties	7
Table 3. Soil layers and foundation properties	8
Table 4. Soil properties	8
Table 5. Soil models and parameters, lateral and axial.....	8
Table 6. Soil models and parameters, torsional and tip	9
Table 7. Pier ultimate capacities, linear-elastic modeling	14
Table 8. Pier ultimate capacities, nonlinear modeling	15
Table 9. Pier ultimate capacities, foundation modeling.....	15
Table 10. Pier ultimate capacities	16

LIST OF ABBREVIATIONS

Item	Definition
AASHTO	American Association of State and Highway Transportation Officials
Elev.	Elevation
FHWA	Federal Highway Administration
ft	Foot
in	Inch
lb	Pound
kip	Kilopound (1,000 pounds)
ksi	Kips per square inch
LRFD	Load and resistance factor design
MHW	Mean high water
NTSB	National Transportation Safety Board
pci	Pounds per cubic inch
pcf	Pounds per cubic foot
psf	Pounds per square foot

FEDERAL HIGHWAY ADMINISTRATION (FHWA) ROLE

The Francis Scott Key Bridge collapse investigation is being led by the National Transportation Safety Board (NTSB). The Federal Highway Administration (FHWA) is supporting NTSB in its investigation by providing resources and expertise on the design, construction, and inspection of highway bridges.

REPORT PURPOSE

This report is the result of FHWA's efforts to determine the capacities of Piers 16 to 19 of the Francis Scott Key Bridge to resist vessel impact loads. These analyses were conducted in support of NTSB's efforts to conduct a post hoc vessel allision risk assessment of the main spans of the bridge in accordance with the Method II analysis described in the *AASHTO Guide Specifications and Commentary for Vessel Collision Design of Highway Bridges*, hereafter referred to as the AASHTO guide specifications.

ANALYSIS METHODS

The ultimate lateral capacity of a pier is the minimum lateral load at which a component (column, cap beam, foundation) reaches a limit state at which the pier is no longer expected to be able to support the bridge superstructure. To determine this capacity, computational models of the pier are subjected to incrementally increasing lateral loads until the limit state under consideration is reached.

The following software packages were used to analyze the piers:

- LARSA 4D – Used to conduct linear and nonlinear structural analyses of the pier structures (columns, struts, and cap beams).
- FB-MultiPier – Used to conduct nonlinear analyses of the pier foundations.
- Microsoft Excel – Use to conduct model development and verification calculations.

Capacities of the pier elements were calculated considering both linear-elastic and nonlinear behavior. Pushover analysis was used to establish the global load-deformation performance of the pier structures considering nonlinear material behavior. Foundation capacities were calculated considering nonlinear load-deformation characteristics of the underlying soils.

As the lateral stiffness of the superstructure, with respect to that of the substructure, was unlikely to substantially contribute to the response to vessel collision loading, each pier was modeled individually to reduce model complexity. Similarly, as the vessel collision demand is applied as a pseudo-static load, it was felt unnecessary to consider coupling of the structural and foundation responses and those components were also modeled independently.

LOADS

The capacity of an axially loaded element to resist bending moments and shears from laterally applied loads is dependent on the level of axial load in the element. This required the calculation of dead and live loads applied to the piers from the both the superstructure and their own weight.

Dead Load

Superstructure dead loads at each pier were calculated using information from the original as-built plans for the bridge. Dead load reactions from the continuous truss spans were calculated from geometric, loading, and member force data provided on the as-built plans:

- Reactions at Piers 16 and 19: 1,023 kips per truss
- Reactions at Piers 17 and 18: 11,028 kips per truss

Dead load reactions at Piers 16 and 19 from the continuous steel girder approach spans were calculated by hand using dimensional information from the as-builts and commonly recognized material unit weights (150 lb/ft³ for concrete, 490 lb/ft³ for steel):

- Reactions at Piers 16 and 19: 1,285 kips

Substructure dead load weights were calculated by hand using dimensions taken from the as-built plans and used to verify results calculated by the structural analysis model. From this, the total dead load axial force in each pier column, at their base, was calculated as:

- Piers 16 and 19: 4,088 kips/column
- Piers 17 and 18: 7,951 kips/column

Dead loads applied to the pile cap in the foundation model would also include the weight of the column pedestals and shear walls and were calculated as:

- Piers 16 and 19: 12,617 kips
- Pier 17 (cap elevation -23.5'): 41,709 kips
- Pier 18 (cap elevation -20.5'): 41,126 kips

Live Load

The application of additional axial load increases the resistance of the elements of interest to this study (the pier columns and foundations) to lateral load demands. For this reason, and the low likelihood of the concurrence of the design vehicular live load and vessel collision load, live load was conservatively taken as zero.

Application of loads

Superstructure dead loads were applied to the pier structure model as vertical point loads placed at the location of the truss bearings. For the foundation model, dead loads from the super- and substructure were applied to the pile caps at the location of the pier columns.

Lateral ship collision loads were applied to a single column of each substructure. According to the AASHTO guide specifications, lateral ship collision loads are to be applied according to the following criteria¹:

1. As a concentrated force on the substructure at the mean high water (MHW) level of the waterway to design the substructure for overall stability, and
2. As a vertical line load equally distributed along the ship's bow depth to design the pier and substructure for local collision forces.

A wide variety of ship classes and sizes are to be evaluated in the risk analysis. To accommodate this, lateral loads were applied at the extremes of the ship bow depths provided in the AASHTO guide specifications, Tables 3.5.2-1 through 3.5.2-3, in an effort to bound the solution. At Piers 17 and 18, this resulted in loads being applied at elevations +28.5' and +57.5'. At Piers 16 and 19, the shallowness of the channel would limit the range of ships that would be likely able to impact the pier, resulting in loads being applied at elevations +32.8' and +50.5'. At each of these elevations, the pier columns were evaluated with the vessel collision load being applied as both a concentrated force and as a distributed line load along the ship's bow depth.

For the foundation analysis, lateral loads were applied as a concentrated load directly to the pile cap.

LIMIT STATES AND LOAD AND RESISTANCE FACTORS

The Extreme Event II limit state was used to analyze the piers. For that limit state, demand is calculated as:

$$Q = \gamma_{DC}DC + \gamma_{CV}CV$$

Where: DC = dead load of structural components and nonstructural attachments

CV = vessel collision force

γ_{LL} = load factor for dead loads

γ_{CV} = load factor for vessel collision loads

For this study, both γ_{DC} and γ_{CV} were taken as 1.0. The use of $\gamma_{DC} = 1.0$ is taken from Table 3.4.1-1 of the *AASHTO LRFD Bridge Design Specifications, 9th Edition*. This differs from the values (1.25 maximum, 0.9 minimum) presented in Article 3.14 of the AASHTO guide specifications but is from a more current document.

Element resistance is calculated as:

$$R_r = \phi R_n$$

¹ *AASHTO Guide Specifications and Commentary for Vessel Collision Design of Highway Bridges*, Second Edition, 2009, Article 3.15.1.

Where: R_r = factored resistance
 R_n = nominal resistance
 ϕ = resistance factor

For this study, consistent with the *AASHTO LRFD Bridge Design Specifications*, the resistance factors at the Extreme Event II limit state were taken to be 1.0.

MATERIAL PROPERTIES

Concrete and Steel

Concrete and steel material models were based on the strengths specified on the as-built plans. As the columns lacked confining reinforcing details, the concrete was modeled as unconfined using a Hognestad parabolic model with the following properties:

Table 1. Concrete properties

Property	Value
Modulus of elasticity (ksi)	3,122
Specified compressive strength, (ksi)	3
Crushing strain (in/in)	0.005
Ultimate tensile strain (in/in)	0

Reinforcing steel was modeled as an elastic-perfectly plastic material without strain hardening using the following properties:

Table 2. Reinforcing steel properties

Property	Value
Modulus of elasticity (ksi)	29,000
Yield stress, (ksi)	40
Ultimate strain (in/in)	0.12

Foundation soils

Soil properties for the analysis were established using available soil borings from the original bridge construction. Based on the available soils information, the following foundation and soils information were used in the model:

Table 3. Soil layers and foundation properties

Location	Pier 16	Pier 17	Pier 18	Pier 19
Elevation, ft				
Top of pile cap	-15.0	-23.5	-20.5	-15.0
Bottom of pile cap	-21.0	-33.5	-30.5	-21.0
Mudline, top of organic clay layer	-20.0	-41.0	-26.0	-25.0
Bottom of organic clay layer	-95.0	-121.0	-91.0	-82.0
Bottom of Upper Patapsco formation	--	--	-106.0	-
Top of Lower Patapsco formation (bearing layer)	-95.0	-121.0	-106.0	-82.0
Pile tip	-110.0	-137.0	-119.0	-112.0
Pile Information				
Steel pile type	HP 14x102	HP 14x102	HP 14x102	HP 14x102
Pile capacity, tons	120	120	120	120

Table 4. Soil properties

Material	Unit Weight, pcf	Friction Angle, degrees	Cohesion, psf	Horizontal Subgrade Modulus, k, pci	Strain, E50
Organic Clay	90	0	100 psf	10 pci	0.02
Upper Patapsco Formation	125	34	0	60	0
Patapsco Formation (bearing layer)	135	38	0	150	0

Table 5. Soil models and parameters, lateral and axial

Material	Lateral		Axial		
	Model	Undrained Shear Strength, C _u , psf	Model	Small Strain Shear Modulus, ksi	Nominal Unit Skin Friction, psf
Organic Clay	Clay-Soft Matlock	100	Driven Pile McVay	0.6	100
Upper Patapsco Formation	Sand-O'Neill	-	Driven Pile McVay	1.5	500
Patapsco Formation (bearing layer)	Sand-O'Neill	-	Driven Pile McVay	2.0	700

Table 6. Soil models and parameters, torsional and tip

Material	Torsional			Tip		
	Model	Shear Modulus, ksi	Torsional Shear Stress, psf	Model	Small Strain Shear Modulus, ksi	Nominal Tip Resistance, kips
Organic Clay	Hyperbolic	0.6	100	Driven Pile McVay	0.6	-
Upper Patapsco Formation	Hyperbolic	1.5	500	Driven Pile McVay	1.5	-
Patapsco Formation (bearing layer)	Hyperbolic	2.0	700	Driven Pile McVay	2.0	400

MEMBER CAPACITIES

The capacity of each pier structure to resist lateral loads is controlled by the ultimate capacity of the pier columns, specifically the voided column sections present in all of the columns in Piers 16 through 19. The capacity of those column sections is based on reaching one of the following limit states:

Column flexural capacity – linear-elastic model

Nominal flexural capacity for liner-elastic modeling was determined via spreadsheet using strain compatibility, with failure being established as the point where strains at the compression face of the column reach 0.003.

The following is the axial load-moment interaction diagram for the voided column sections in Piers 16 and 19:

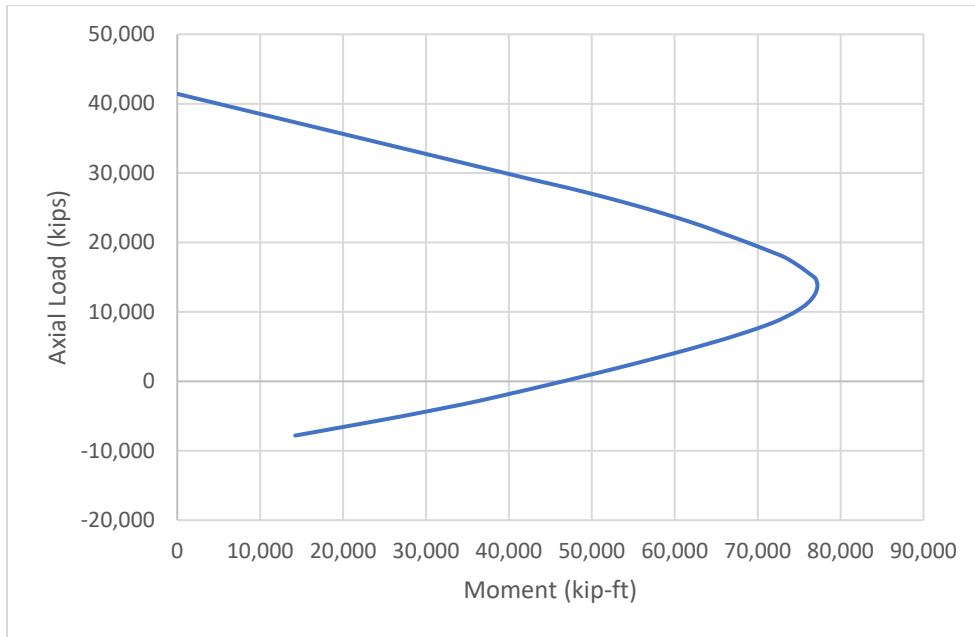


Figure 1. Axial load-moment diagram, Piers 16 and 19 section with void

The following is the axial load-moment interaction diagram for the voided column section at Pier 17 and 18:

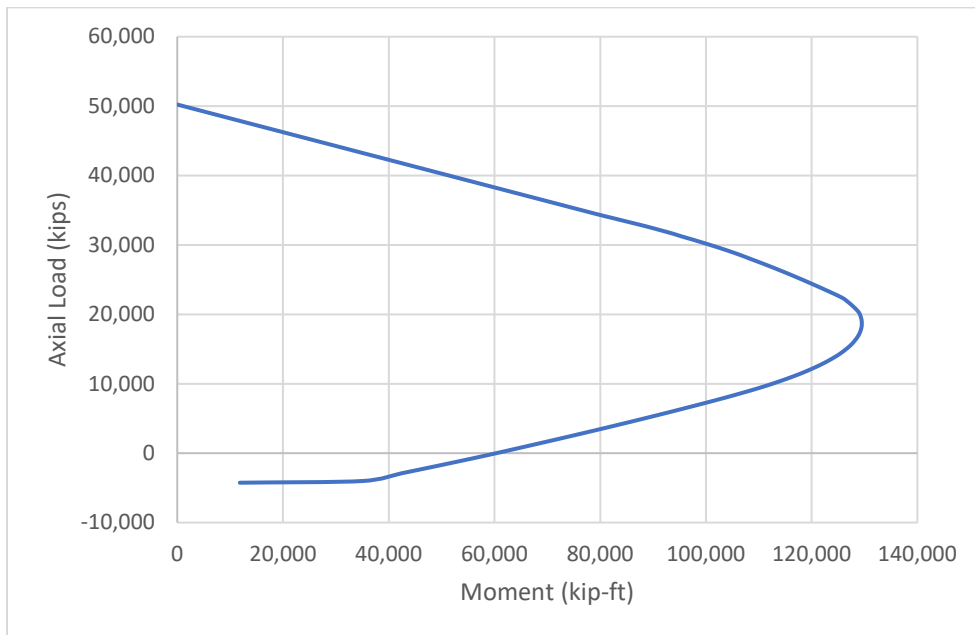


Figure 2. Axial load-moment diagram, Piers 17 and 18 section with void

Column flexural capacity – nonlinear model

Rotational stiffness and ultimate flexural capacity of the column are the key characteristics required for pushover analysis and are expressed in terms of the moment-curvature relationship.

Moment-curvature is axial load dependent, and so is calculated by the modeling software at each increment of the pushover analysis as the application of lateral loads to the pier redistribute axial loads in the columns. To verify the behavior of the LARSA 4D model, the moment-curvature relationship under only dead load was calculated in a spreadsheet using strain compatibility and compared to output from LARSA 4D. Good agreement was demonstrated for both the Piers 16 and 19 and the Piers 17 and 18 column models:

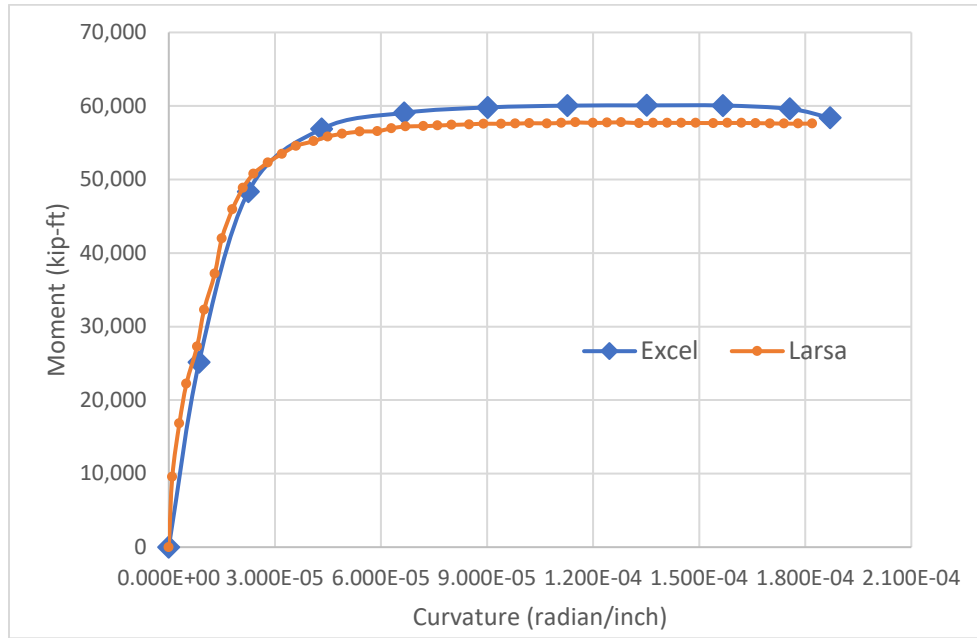


Figure 3. Moment-curvature relationship for Piers 16 and 19 at axial load, P = 4,088 kips

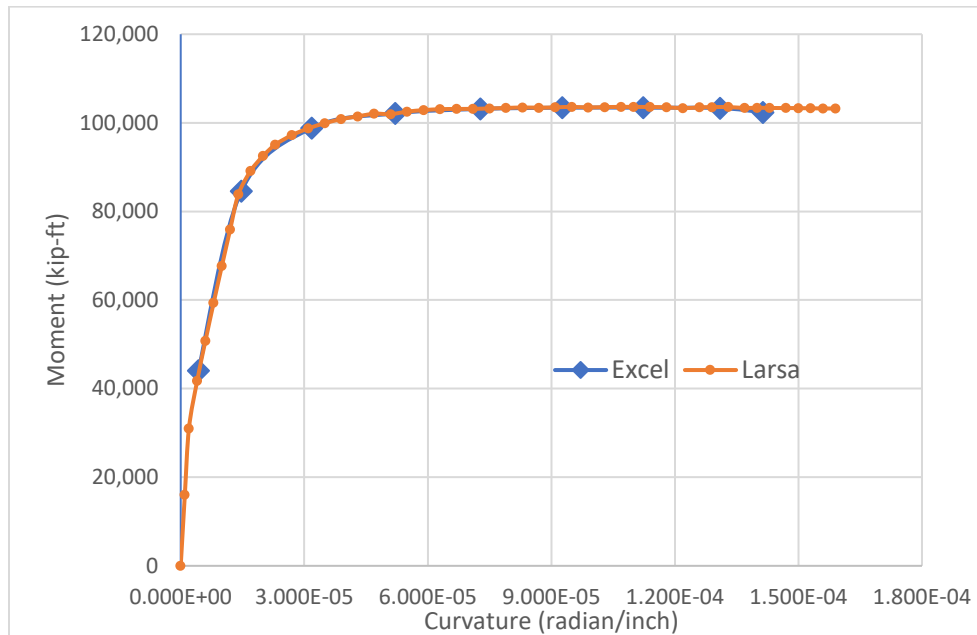


Figure 4. Moment-curvature relationship for Piers 17 and 18 at axial load, P = 7,951 kips

Column shear capacity

The as-built plans for Piers 16 through 19 indicated the presence of a construction joint at the base of the columns at the transition between the solid and voided sections:

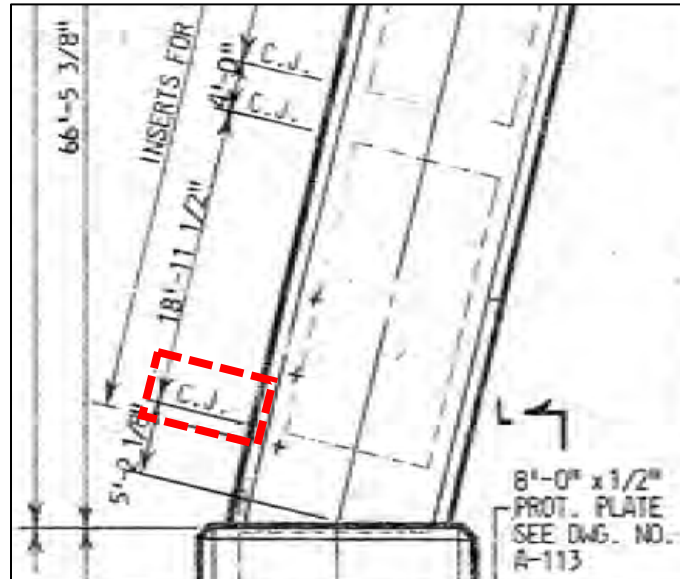


Figure 5. As-built drawing of Pier 18 showing column construction joint (noted “C.J.”)

The presence of these construction joints, and the large change in sectional area at those construction joints indicate that interface shear, rather than flexural shear, is the appropriate failure mechanism to consider at the base of the columns. The *AASHTO LRFD Bridge Design Specifications*, 9th Edition, provides the following equation (Equation 5.7.4.3-3) for calculating interface shear capacity:

$$V_{ni} = cA_{cv} + \mu(A_{vf}f_y + P_c)$$

Where: c = cohesion factor

A_{cv} = surface area of the shear interface

μ = friction factor

A_{vf} = area of reinforcing steel crossing the interface

f_y = reinforcing steel yield strength

P_c = permanent net compressive force normal to the shear plane

The cohesion and friction factors vary based on the characteristics of the interface. It is unknown to what degree the construction joint surfaces were prepared during bridge construction, so conservative values were assumed for this analysis. Considering the inclination of the interface and expected cracking of the column ends under lateral load, cohesion along the interface was considered to be unreliable and c was taken as zero. The friction coefficient was taken as 0.6,

representing “concrete placed against a clean concrete surface, free of laitance, but not intentionally roughened.”²”

The as-built drawings indicated that the longitudinal reinforcing bars in the column were lap spliced at or near the interface. Detailed bar tables were not available for the piers, making it unclear to what length the bars were spliced. The transverse steel in the columns was detailed such that these splices were not fully enclosed in the hooks of the lateral reinforcing. The unknown lap splice length and lack of confinement cast doubt on the ability of those bars to achieve their full yield strength, as is assumed in the interface shear equation, and thus their contribution to the interface shear capacity was ignored.

These considerations simplify the capacity calculation to $V_{ni} = \mu P_c = 0.6P_c$, resulting in the following shear capacities under dead load alone:

- Piers 16 and 19: 2,453 kips
- Piers 17 and 18: 4,771 kips

These capacities were considered as a limit state in both the linear-elastic and nonlinear models.

PIER CAPACITY CALCULATIONS

Linear-elastic modeling

From the above, both the axial and interface shear capacity of the columns are dependent on axial load in the column. The application of lateral load to the pier will result in overturning moments creating axial load couples that lead to higher axial loads in some columns and lower axial loads in others, compared to dead load alone. Thus, an iterative approach was used to determine lateral load capacity, where applied lateral loads were adjusted to achieve agreement between resultant axial loads in the columns and their calculated capacities. The load at which this agreement was reached became the reported linear-elastic ultimate capacity. This process resulted in the following ultimate pier capacities:

² AASHTO LRFD Bridge Design Specifications, 9th Edition, Article 5.7.4.4

Table 7. Pier ultimate capacities, linear-elastic modeling

Location	Scenario	Failure Mode	Capacity, Applied as Point Load (kips)	Capacity, Applied as Distributed Load (kips)
Pier 16	Higher load application (Elev. 50.5)	Interface Shear	3,816	6,207
		Flexure	4,972	18,547
	Lower load application (Elev. 32.8)	Interface Shear	3,045	8,880
		Flexure	8,498	60,012
Pier 17	Higher load application (Elev. 57.5)	Interface Shear	7,282	13,041
		Flexure	6,877	23,343
	Lower load application (Elev. 28.5)	Interface Shear	5,539	34,649
		Flexure	13,181	43,694
Pier 18	Higher load application (Elev. 57.5)	Interface Shear	7,230	12,417
		Flexure	7,019	23,451
	Lower load application (Elev. 28.5)	Interface Shear	5,501	31,657
		Flexure	13,881	45,620
Pier 19	Higher load application (Elev. 50.5)	Interface Shear	3,816	6,207
		Flexure	4,972	18,547
	Lower load application (Elev. 32.8)	Interface Shear	3,045	8,880
		Flexure	8,498	60,012

Lower pier capacities for point loads applied at the lower elevation reflect the proximity of the applied load to the controlling point of interest (the base of the column), and less redistribution of lateral load to the other pier columns. Higher calculated pier capacities for the application of lateral loads as a distributed load are a result of that load also being applied to additional elements (i.e., the column pedestals), with higher resistances.

Nonlinear modeling

Nonlinear pushover analyses resulted in the following ultimate pier capacities:

Table 8. Pier ultimate capacities, nonlinear modeling

Location	Scenario	Failure Mode	Capacity, Applied as Point Load (kips)	Capacity, Applied as Distributed Load (kips)
Pier 16	Higher load application (Elev. 50.5)	Interface Shear	4,710	6,597
		Flexure	9,039	26,358
	Lower load application (Elev. 32.8)	Interface Shear	3,219	9,676
		Flexure	11,298	58,909
Pier 17	Higher load application (Elev. 57.5)	Interface Shear	7,645	12,292
		Flexure	8,856	34,569
	Lower load application (Elev. 28.5)	Interface Shear	5,509	33,604
		Flexure	21,729	65,368
Pier 18	Higher load application (Elev. 57.5)	Interface Shear	7,592	11,872
		Flexure	8,849	35,848
	Lower load application (Elev. 28.5)	Interface Shear	5,459	31,607
		Flexure	19,544	70,930
Pier 19	Higher load application (Elev. 50.5)	Interface Shear	4,710	6,597
		Flexure	9,039	26,358
	Lower load application (Elev. 32.8)	Interface Shear	3,219	9,676
		Flexure	11,298	58,909

Calculated pier displacements at the ultimate capacity (taken at the point of applied load) varied from 0.3” to 4.3”, with the lower displacement capacities being associated with shear failure at the base of the columns.

FOUNDATION CAPACITY CALCULATIONS

Foundation capacities were determined as the minimum applied lateral load at which demand in the foundation H-piles exceeds their capacity. This resulted in the following ultimate pier capacities:

Table 9. Pier ultimate capacities, foundation modeling

Location	Scenario	Failure Mode	Capacity, (kips)
Pier 16	Foundation	H-pile failure	1,908
Pier 17	Foundation	H-pile failure	6,360
Pier 18	Foundation	H-pile failure	7,560
Pier 19	Foundation	H-pile failure	1,920

DISCUSSION AND REPORTED CAPACITIES

In all loading cases, the capacity of the columns at Piers 16 and 19 were controlled by reaching the interface shear capacity at the base of the columns. At Piers 17 and 18, linear-elastic capacities for loads applied higher on the pier were controlled by flexure, and lower on the pier by interface shear. These capacities were associated with small displacements at the point of applied load, reflecting a low ability for the piers to behave in a ductile fashion and absorb kinetic energy from a vessel collision. The application of the vessel collision load as a distributed force assumes a substantial amount of ship bow deformation, which the non-ductile pier load-deformation response indicates is unachievable. For this reason, it is felt that capacities calculated from applying the vessel collision force as a point load, representing a bow strike, are more realistic.

At Piers 16 and 19, the foundations were shown to reach their ultimate capacity prior to the pier columns reaching their ultimate capacity. Therefore, the controlling capacities for those piers reflect the foundation capacity.

The capacities recommended for use in the Method II analysis are as follows:

Table 10. Pier ultimate capacities

Location	Lateral Load Capacity	Mode of Failure
Pier 16	1,908 kips	Foundation H-pile
Pier 17	5,509 kips @ Elev. 28.5'	Column base shear (interface), nonlinear response
	6,877 kips @ Elev. 57.5'	Column base moment, linear-elastic response
Pier 18	5,459 kips @ Elev. 28.5'	Column base shear (interface), nonlinear response
	7,019 kips @ Elev. 57.5'	Column base moment, linear-elastic response
Pier 19	1,920 kips	Foundation H-pile